LIMNOLOGY and OCEANOGRAPHY

ASLO

Limnol. Oceanogr. 66, 2021, 4077–4095

doi: 10.1002/lno.11944

Environmental gradients and physical barriers drive the basin-wide spatial structuring of Mediterranean Sea and adjacent eastern Atlantic Ocean prokaryotic communities

Marta Sebastián,[1*] **Eva Ortega-Retuerta**,[2] **Laura Gómez-Consarnau**,[3,4] **Marina Zamanillo**,[1,5] **Marta Álvarez**,[6] **Javier Arístegui**,[7] **Josep M. Gasol**[1,8*]

[1]Institut de Ciències del Mar, CSIC, Barcelona, Catalunya, Spain
[2]CNRS/Sorbonne Université, UMR7621 Laboratoire d'Océanographie Microbienne, Banyuls sur Mer, France
[3]Centro de Investigación Científica y de Educación Superior de Ensenada, Ensenada, Baja California, Mexico
[4]Department of Biological Sciences, University of Southern California, Los Angeles, California
[5]Instituto Español de Oceanografía, Centre Oceanogràfic de les Balears, Palma, Spain
[6]Instituto Español de Oceanografia, Centro Oceanográfico de A Coruña, A Coruña, Galicia, Spain
[7]Instituto de Oceanografía y Cambio Global, IOCAG, Universidad de Las Palmas de Gran Canaria, ULPGC, Gran Canaria, Spain
[8]Centre for Marine Ecosystems Research, School of Sciences, Edith-Cowan University, Joondalup, Western Australia, Australia

Abstract

The Mediterranean Sea is a miniature ocean divided by the Sicily Strait into two basins with a marked west to east trophic gradient and separated of the nearby eastern Atlantic Ocean by the Strait of Gibraltar. Here, we test the hypothesis that these physical and environmental barriers favor the development of specific prokaryotic assemblages, leading to changes in community structure both in the vertical and horizontal spatial scales. By analyzing taxonomic and phylogenetic diversity using amplicon sequence variants (ASVs) of the 16S rRNA gene, we show that there is indeed marked vertical segregation of prokaryotic groups, similar to that found in other areas of the ocean, but also a clear horizontal structuring among the two Mediterranean basins and the adjacent Atlantic waters. Prokaryotic diversity increased with depth and toward the Atlantic, whereas the easternmost stations displayed more phylogenetically diverse phylotypes, despite harboring globally less diverse communities. Basin-indicator taxa (ASVs) accounted for a large fraction of the community (between 50% and 80%) in each of the basins at the surface and bathypelagic layers, being associated with different environmental variables. The existence of biogeographic and environmental barriers in the Mediterranean Sea is likely related to the trophic gradient at the surface and the isolation of water bodies in depth due to the Gibraltar and Sicily straits. Our work highlights the importance of studying microbial regional biogeography and provides the basis for future studies on the impact of this regionalization in the function of Mediterranean Sea prokaryotic communities.

With a global abundance of ca. 1.2×10^{29} cells (Whitman et al. 1998), marine prokaryotes (bacteria and archaea) drive most biogeochemical transformations in our planet (Falkowski et al. 2008). The advent of molecular methods, allowing to obtain large datasets at relatively low costs, has shown that marine microbes comprise a vast diversity and a myriad of metabolic capabilities. Marine prokaryotes are key mediators in a broad range of elemental cycles and thus, knowing their biogeography is critical to develop a predictive understanding of microbial processes in the ocean and how they will evolve in future global change scenarios. Despite the profusion of microbial biogeographic studies (Herlemann et al. 2011; Sunagawa et al. 2015; Milici et al. 2016) there are still ocean areas that are far from being well-known. For instance, studies looking at prokaryotic composition and its variability in the dark ocean are limited (but see Agogué et al. 2011; Salazar et al. 2015), even though dark ocean waters (> 200-m depth) host 70% of ocean's prokaryotic cells (Arístegui et al. 2009).

*Correspondence: msebastian@icm.csic.es; pepgasol@icm.csic.es

Additional Supporting Information may be found in the online version of this article.

Author Contribution Statement: M.S. and E.O.-R. contributed equally to the work.

Microbial biogeographic patterns result from speciation, extinction, and dispersal processes that lead to a combination of cosmopolitan and endemic species in different regions (Hanson et al. 2012). In ocean ecosystems, dispersal limitation is often determined by the existence of physical barriers such as straits or islands, different water masses, currents, or fronts, which highly determine prokaryotic community structure (Baltar and Arístegui 2017; Morales et al. 2018). On the other hand, environmental factors such as temperature, inorganic and organic nutrients, or sunlight highly constrain prokaryotic community structure by imposing niche differentiation (Coleman and Chisolm 2010; Gilbert et al. 2011; Sunagawa et al. 2015).

The Mediterranean Sea, with a total area of 2.5×10^6 km^2, is the largest semi-enclosed basin on Earth. It is frequently treated as a miniature ocean because it has its own overturning circulation, and relevant oceanographic processes, such as dense water formation, occur in this basin (Bethoux et al. 1999). Globally oligotrophic, it presents a west to east gradient of increasing oligotrophy (Krom et al. 1991), with growth and activity of microbial communities inhabiting the euphotic Mediterranean Sea being generally limited by phosphate availability (Thingstad et al. 1998; Pinhassi et al. 2006). Exclusive from the Mediterranean Sea are also the high salinity (38–39 relative to ca. 35 in the open ocean) and the relatively high temperatures in the meso- and bathypelagic layers (about 10°C warmer than deep waters of the global ocean) that appear to lead to higher remineralization rates compared to other deep ocean basins (Christensen et al. 1989; Santinelli et al. 2010). One of the main physical features of this basin is that it is connected to the adjacent Atlantic Ocean only by the shallow and narrow Strait of Gibraltar (300 m deep, 13 km wide). This physical barrier reduces water mixing and promotes an inflow of surface nutrient-poor waters from the Atlantic to the Mediterranean Sea that outweighs the outflow of nutrient-rich deep waters in the opposite direction (Sammartino et al. 2015). In addition, the strait of Sicily (500 m deep) divides the Mediterranean Sea into two basins, the Western and Eastern Mediterranean, physically isolating the deep water bodies from both basins. The existence of these barriers led us to hypothesize that prokaryotic community structure in the Mediterranean Sea must be impacted by a combination of these physical barriers (i.e., prokaryotic communities will be more disconnected in the meso- and bathypelagic basins than in the euphotic layers) together with other environmental parameters, namely the west-to-east and vertical gradients in substrate availability.

Most published studies looking at biogeographic patterns of prokaryotic communities using state-of-the-art high-throughput sequencing of the 16S rRNA gene in the Mediterranean Sea have focused in a few localized areas (reviewed in Pulido-Villena et al. 2012; Luna 2014): the coastal Tyrrhenian (Thiele et al. 2017), the NW Mediterranean Sea (Laghdass et al. 2010; Crespo et al. 2013; Severin et al. 2016; Mestre et al. 2017), the Ligurian Sea (Celussi et al. 2018), the Adriatic (Korlević et al. 2015), and, to a lesser extent, the Eastern Mediterranean Sea (De Corte et al. 2009; Yokokawa et al. 2010; Techtmann et al. 2015). To date, the broad-scale patterns of prokaryotic diversity and community composition in this enclosed sea have only been studied once using automated ribosomal intergenic spacer analysis (ARISA) fingerprinting (Mapelli et al. 2013, which found a longitudinal and vertical structuring of prokaryotic communities, but lacked information on the taxonomic composition of these communities.

To explore the role of the geographic barriers and the oceanographic gradients in structuring prokaryotic communities in the Mediterranean Sea, we present a quasi-synoptic view of the basin-wide distributions of archaeal and bacterial communities using 16S rRNA gene illumina sequencing. We collected samples on a transect that covered the most representative regions and water masses of the Mediterranean Sea in the opposite direction to the surface Atlantic water flow, from east to west, and from surface to near-bottom waters, including the adjacent Eastern North Atlantic Ocean. Complementing these data with a large dataset of ancillary environmental parameters, we investigated the main physical and environmental factors driving prokaryotic diversity as well as the determinants of spatial differentiation. The main hypotheses addressed were: (1) the west–east gradient in oligotrophy is reflected by a west to east decreasing trend in prokaryotic diversity; and (2) the combination of physical barriers (i.e. the Gibraltar and Sicily straits) and the sharp changes in environmental parameters segregate prokaryotic communities by depth and basin.

Methods

Seawater sampling was carried out during the HOTMIX 2014 cruise on board the *R/V Sarmiento de Gamboa*, from 29 April to 28 May 2014. Seawater was collected at 29 stations along a Mediterranean Sea section from east to west, also extending to the adjacent subtropical northeast (NE) Atlantic Ocean reaching the Canary Islands (Fig. 1). Detailed information about the distributions of salinity, potential temperature and chlorophyll *a* (Chl *a*) concentrations as well as the water masses intercepted during the cruise is provided in Catalá et al. (2018). Samples were collected using a rosette sampler holding 24 Niskin bottles (12 liters each), coupled to a Seabird SBE 9-11 plus conductivity-temperature–pressure probe, complemented with a SBE43 oxygen sensor and a SeaTech fluorometer. Up to 13 depths were sampled covering the entire water column, from 3 m down to 10 m above the seafloor.

Samples from the epipelagic layer (surface water; down to 200 m) were systematically collected at four depths: 3 m, the depth receiving 20% of the surface photosynthetically active radiation, the depth of the deep chlorophyll maximum (DCM), and between 10 and 45 m below the DCM. The depth of the DCM was determined after visual inspection of the

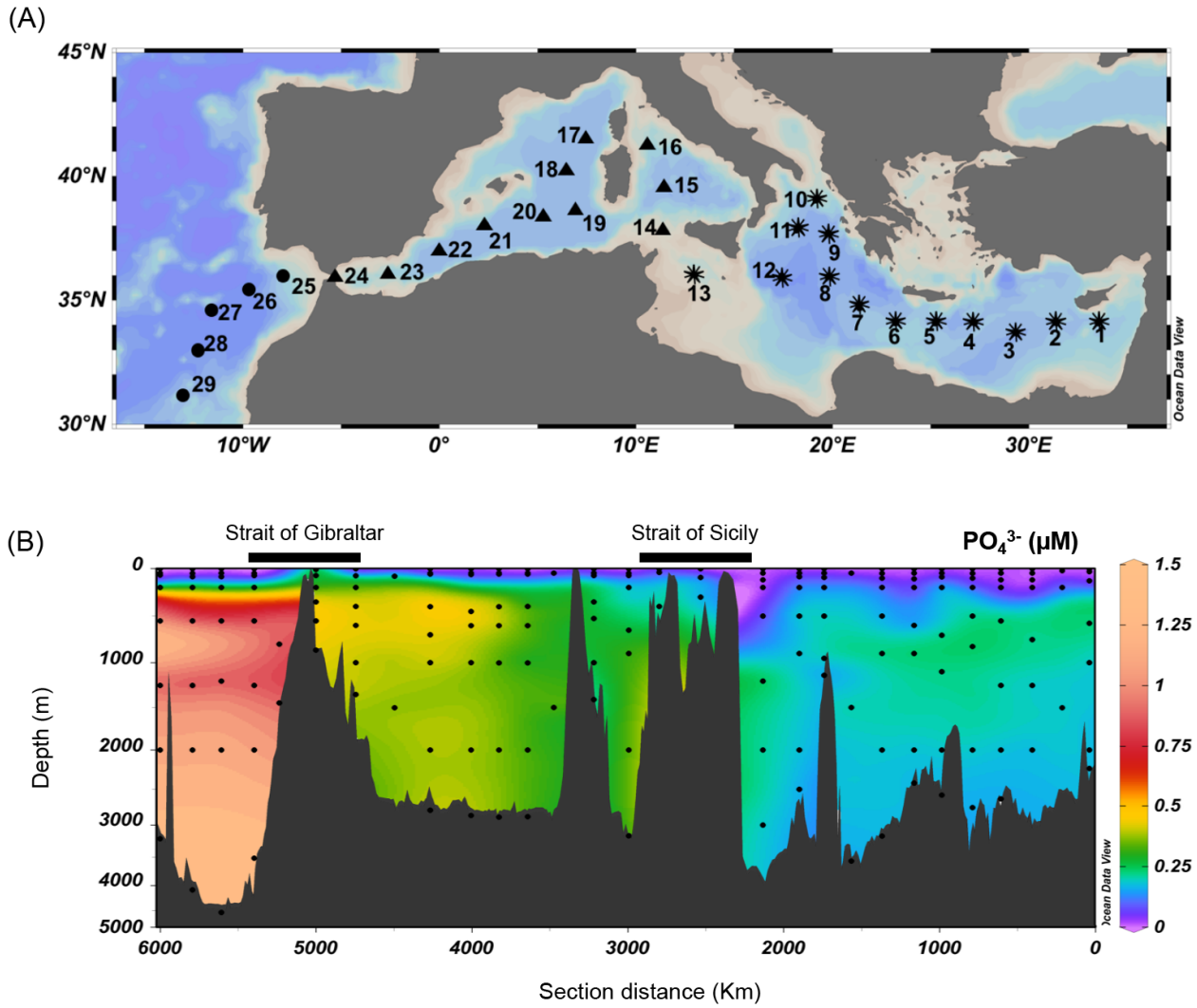

Fig 1. (**A**) Study area and stations sampled during the HOTMIX2014 cruise, different symbols correspond to the different basins (dots: Atlantic; triangles: Western Med. basin; asterisks: Eastern Med. basin). (**B**) Vertical profile showing the Gibraltar and Sicily straits that act as physical barriers in the dark Mediterranean Sea. Dots represent the samples collected for prokaryotic diversity. The color contour plot shows the vertical distribution of phosphate concentration along the transect.

vertical profiles of Chl *a* fluorescence. Sampling depths in the meso- and bathypelagic layers were chosen according to the full-depth potential temperature, salinity, and dissolved oxygen profiles, to ensure that all the water masses of the Mediterranean Sea and their respective mixing zones were sampled (for more details, see Catalá et al. 2018). In this study, we discriminated mesopelagic from bathypelagic samples using the global criterion of 1000 m depth (sample from 200 to 1000 m were considered mesopelagic and samples deeper than 1000 m were considered as bathypelagic).

Environmental variables

Dissolved oxygen, inorganic nutrients (nitrogen, phosphorus, and silicate), Chl *a*, total and particulate organic carbon, particulate organic nitrogen, colored and fluorescent dissolved organic matter (DOM), transparent exopolymer particles, heterotrophic prokaryotic abundance (PA), and the percentage of high nucleic acid cells were determined in discrete samples using standard protocols as described elsewhere (Catalá et al. 2018; Martínez-Pérez et al., 2019; Ortega-Retuerta et al. 2019). For a brief description on the methodologies, see Supporting Information Methods.

Nucleic acids extraction

Samples for nucleic acids extraction (4–12 liters) were sequentially filtered through 47-mm 3-μm polycarbonate membrane filters (Merk Millipore, Isopore polycarbonate) and 0.2-μm pore size Sterivex units with a peristaltic pump. Total nucleic acids from the 0.2–3-μm size fraction were extracted using the PowerWater Sterivex™ DNA isolation Kit (MO BIO Laboratories) following the manufacturer instructions. DNA was quantified using a Qubit fluorometer assay (Life

Technologies). The V4-V5 region of the 16S gene was amplified with the primers 515F and 926R (Parada et al. 2016) and sequenced in an Illumina MiSeq platform using 2×250 bp paired-end approach at the RTLGenomics facility (https://rtlgenomics.com/). The collected samples for nucleic acids are shown in Fig. 1B.

Data analyses

Primers and spurious sequences were trimmed using cutadapt (Martin 2011). DADA2 v1.8 was used to differentiate exact sequence variants (Callahan et al. 2016). DADA2 resolves amplicon sequence variants (ASVs) by modeling the errors in Illumina-sequenced amplicon reads. Taxonomic assignment was performed using the function "assignTaxonomy" against SILVA v.132 through the RDP naive Bayesian classifier method described in (Wang et al. 2007). ASVs assigned to chloroplasts or eukaryotes were removed for subsequent analyses. All raw sequences used in this study are publicly available at the European Nucleotide Archive (PRJEB44474). The ASV table was randomly subsampled down to the minimum number of reads per sample using the "*rrarefy*" function in the Vegan 2.5-5 package (Oksanen et al. 2015) for the nmds ordination, the diversity index estimates, and the indicator ASV analyses (see below).

Data treatment and statistical analyses were performed with the R (version 3.6.0) and RStudio software (version 1.2.1335). The phylogenetic diversity (PD) was calculated considering the evolutionary relationships among ASVs using the computed phylogeny for each sample, as the sum of the lengths of all the branches in the phylogeny. For this, we used the "DECHIPER" 2.14.0 and "phangorn" 2.5.5 packages (Schliep 2011; Wright 2016). Prokaryotic richness (the number of ASV per sample) and sample evenness (using the Pielou index: $J = H/\ln(\text{nASV})$, where H is the Shannon index and nASV is the richness in every sample), were calculated using the "Vegan" 2.5-5 package.

In order to assess to which extent environmental conditions and the physical barriers affect the assembly of the prokaryotic communities, we investigated if there were indicator ASVs from each different basin: North East Atlantic, Western Mediterranean, and Eastern Mediterranean Sea. Indicator taxa were identified using the IndVal index from the "labdsv" 2.0-1 package (Roberts 2019), which takes into account the fidelity and relative abundance of the taxa in the different basins. *p*-Values were adjusted using the false discovery rate approach (Benjamini and Hochberg 1995). Given the vertical stratification of the prokaryotic communities, we calculated the basin-indicator taxa separately for each of the four depth layers studied: surface, DCM, mesopelagic, and bathypelagic.

To test for significant differences in richness, PD, the ratio PD/richness, and evenness, we used one-way ANOVA and post hoc Tukey tests using depth layer and basin as factors. The same statistical tests were applied using the proportion of sequences of each ASV per layer and basin.

Diversity metrics were correlated against the main environmental variables using pairwise Pearson correlations on log10-transformed data, with posterior Bonferroni corrections. Figures were constructed using "ggplot2" 3.2.1 in R.

The association of the basin-indicator ASVs with biotic and environmental variables was explored using a sparse partial least squares (sPLS) regression analysis using the "mixOmics" package (Rohart et al. 2017) in R in "regression" mode. We included the following variables: temperature, salinity, apparent oxygen utilization, nitrate and phosphate concentration, fluorescent dissolved organic matter (FDOM) peaks C (humic-like), and T (protein-like), the spectral slope of chromophoric dissolved organic matter (CDOM) between 275 and 295 nm, total organic carbon (TOC), particulate organic carbon, prokaryotic cell abundance, % high nucleic acid prokaryotes, transparent exopolymer particles concentration, and photic layer integrated (upper 200 m) nitrate and phosphate concentration values. Leave-one-out cross-validation was performed to evaluate model performance (Lê Cao et al. 2008). sPLS allowed the simultaneous selection of meaningful variables in both the basin-indicator ASVs and the environmental dataset, and the resulting pair-wise associations were visualized using clustered image maps (González et al. 2012).

Results

The environmental and biotic parameters monitored along our transect exposed the existence of marked gradients in different regions and depths. While the overall sea surface temperature ranged from 16.3°C to 19.3°C and all stations were thermally stratified (Fig. S1A), Mediterranean deep waters were increasingly warmer toward the Eastern basin, up to 9°C warmer than the Atlantic ones (Fig. S1A). This marked spatial gradient was also observed for salinity, which increased from west to east at all depths of the water column (Fig. S1B), and for inorganic nutrients, where a clear west to east increase in oligotrophy (i.e., decrease in inorganic nutrient concentrations) was evidenced (Figs. 1, S1C). TOC decreased from surface to deep waters and, while TOC in deep waters decreased from west to east, TOC accumulation in the surface occurred in the Eastern basin (Martínez-Pérez et al. 2019; Fig. S1D). PA ranged from 0.21 to 10.2×10^5 cells mL^{-1} and decreased with depth, from an average of 5.12×10^5 cells mL^{-1} in epipelagic waters to an average of 0.42×10^5 cells mL^{-1} in the bathypelagic. PA was lower in bathypelagic waters of the Atlantic and Eastern Mediterranean basins than in bathypelagic Western Mediterranean waters (Fig. S1E).

Besides the clear differences in environmental conditions among the three main basins (i.e., East and West Mediterranean and Atlantic Ocean; Fig. S1), there were sharp differences in some of the subbasins, particularly the Tyrrhenian Sea, which had higher overall temperature, lower salinity, lower nutrients, and higher mesopelagic PA abundances than the westernmost stations in the Mediterranean Sea. Given that

prokaryotic diversity was only sampled in two stations of this subbasin (Sta. #15 and #16), we did not formally compare the different subbasins of the Western Mediterranean.

Prokaryotic community structure and diversity

The taxonomic similarity between samples was assessed by placing them in a two-dimensional space based on nonmetric multidimensional scaling (Fig. 2). Prokaryotic communities were significantly structured by depth layer (PERMANOVA test, $R^2 = 0.43$, $p < 0.001$; Fig. 2; Table S1), and then clustered according to the different basins (PERMANOVA test, $R^2 = 0.07$, $p < 0.001$; Table S1). Differences between basins were also significant when treating the different water layers as separate datasets (PERMANOVA test, $p < 0.001$, $R^2 = 0.39$ for surface, $R^2 = 0.14$ for DCM, $R^2 = 0.30$ for mesopelagic, and $R^2 = 0.41$ for bathypelagic; Table S1).

Prokaryotic richness was on average 396 ASVs per sample, and increased with depth, showing significantly higher values in the meso- and bathypelagic layers than in the euphotic layers (surface and DCM, ANOVA + Tukey HSD post hoc pairwise test, $p < 0.001$; Fig. 3). On the horizontal scale, a significant west to east decrease in richness was also observed (Fig. 3; Table 1). These spatial patterns in richness were also followed by PD (Fig. 3), which ranged widely from 12.2 (Eastern Mediterranean, surface) to 102.2 (Western Mediterranean, mesopelagic; Table 1). In fact, richness and PD were positively correlated (Pearson correlation, $n = 186$, $R = 0.94$, $p < 0.001$). Patches of relatively high richness and PD were observed in NE Atlantic waters around 1300 m, in bottom Western Mediterranean waters next to the Strait of Gibraltar, and in the Ionian sea (Sta. 11 and 12) in the Eastern Mediterranean (Fig. S2). By contrast, PD normalized by richness (PD/rich, an indication of how phylogenetically diverse are the communities normalized by overall richness) was higher in the Eastern Mediterranean (Fig. 3), particularly at the easternmost stations of the Levantine basin (Fig. S2). Sample evenness showed no clear longitudinal or vertical trends, but displayed overall higher values in the mesopelagic (Fig. 3).

The different diversity indices correlated significantly with several environmental variables, particularly in the bathypelagic. In this layer, both richness and PD presented significant positive correlation coefficients with inorganic nutrients, salinity, and the humic-like FDOM peak C (Table S2). In contrast, the PD/richness ratio was significantly negatively correlated with PA and TOC. In the other depth layers, diversity indexes were less influenced by environmental variables, although we found that humic-like FDOM peak C was negatively correlated with the PD/richness ratio in the mesopelagic layer, and positively correlated with evenness at the DCM (Table S2).

Looking at the fraction of shared taxa throughout the water column (considering all ASVs in every basin), we found that overall, around half of the ASVs were exclusively detected in the dark ocean (meso- and bathypelagic layers; Fig. 4), and only 1% of the ASVs was shared among all layers. Microbial communities from the Atlantic displayed a large degree of isolation in the bathypelagic, with 45.2% of the basin ASVs

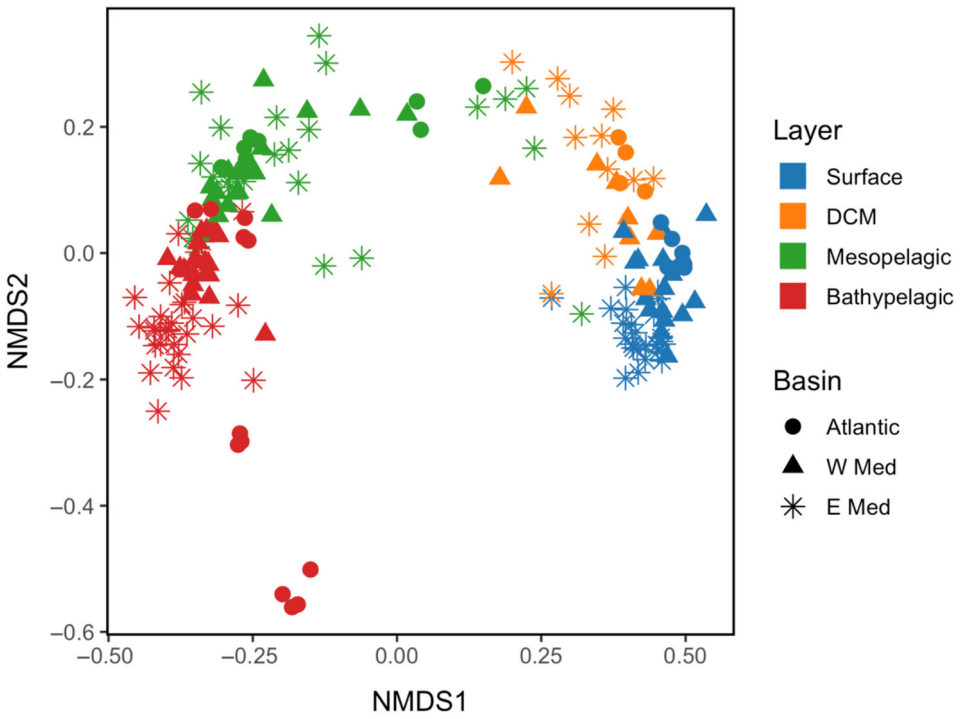

Fig 2. Nonmetric multidimensional scaling (NMDS) ordination based on Bray Curtis similarities of the prokaryotic communities. Color codes separate depth layers. B, Bathypelagic; M, Mesopelagic; DCM, deep chlorophyll maxima; S, surface; symbols denote basins.

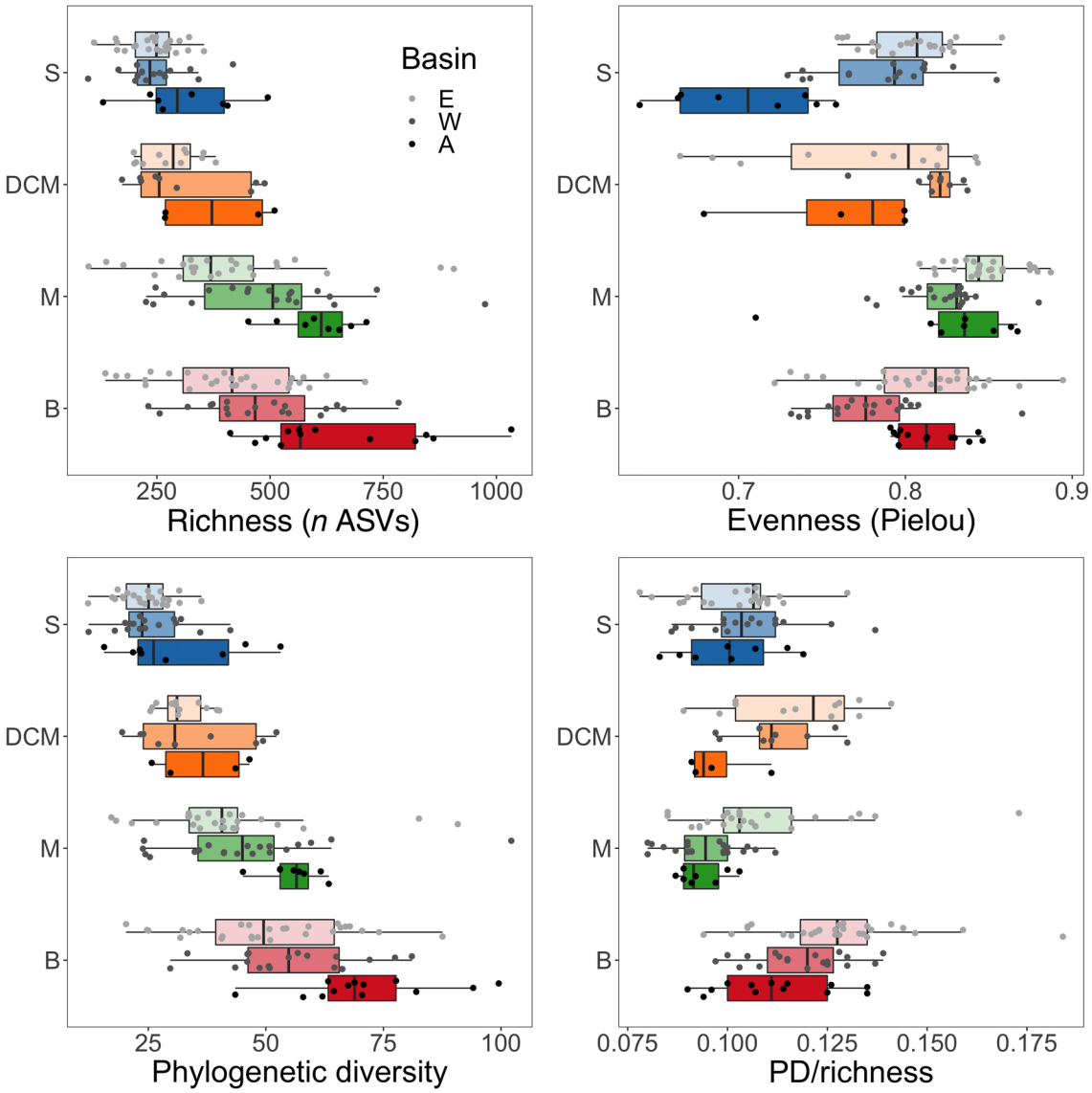

Fig 3. Prokaryotic diversity, expressed as richness (number of ASVs, top left panel), evenness (Pielou index, top right panel), phylogenetic diversity (bottom left panel) and phylogenetic diversity normalized by richness (bottom right panel) by depth layer (S, surface; DCM, deep chlorophyll maxima; M, Mesopelagic; B, Bathypelagic). Whisker transparency represent the ocean basin (E, light colors: Eastern Mediterranean; W, 50% transparency: Western Mediterranean; A, dark colors: Eastern North Atlantic).

exclusively found at this layer. This isolation was less evident for the mesopelagic, where unique ASVs represented 17% of the ASVs. In contrast, the proportion of ASVs exclusively found in meso- and bathypelagic layers were similar in the Mediterranean basins (~ 25% of the ASVs) (Fig. 4). Meso- and bathypelagic layers shared on average 14% of the ASVs, whereas the proportion of ASVs shared between the photic layers (surface and DCM) was on average 4%. In terms of sequences, these unique ASVs were quite rare, as they represented overall a very small proportion of the community (< 7%) (Fig. S3). A clear exception was the Atlantic bathypelagic unique ASVs, which represented on average ~ 40% of bathypelagic communities. This high contribution of unique ASVs, however, was partly due to the deeper waters (> 3000 m) sampled in this basin, where unique ASVs represented up to 80% (data not shown). Considering similar depths to the Mediterranean basins, the contribution of unique ASVs to the Atlantic bathypelagic communities was still significant, around 30%, but more similar to values found in the deeper bathypelagic waters of the Eastern Mediterranean (~ 20%, data not shown).

Spatial changes in the prokaryotic community composition

The bulk taxonomic composition of surface, mesopelagic, and bathypelagic communities was relatively similar throughout the

Table 1. Average (± standard deviation) richness (number of ASVs), phylogenetic diversity, phylogenetic diversity normalized by richness (PD/richness), and evenness (Pielou index) in the different basins and depth layers. n = number of samples. Letters denote significant differences ($p < 0.05$) between basins after one-way ANOVA and post hoc Tukey tests.

		Surface	DCM	Mesopelagic	Bathypelagic	All layers
Richness	Atlantic	313±116a	380±130a	602±86a	650±188a	524±203a
	Western Med	246±74a	312±124a	489±186ab	480±146b	401±177b
	Eastern Med	243±59a	280±65a	405±192b	407±151b	345±156b
	Global	256±78	308±102	467±189	483±181	
Phylogenetic diversity	Atlantic	31.5±13.3a	36.4±10.2a	55.9±5.7a	70.9±14.8a	53.6±20.5a
	Western Med	25.5±7.4a	34.7±12.6a	45.6±17.9a	55.7±13.9b	42.0±18.0b
	Eastern Med	24.5±5.5a	32.1±5.1a	41.6±16.7a	50.3±16.5b	38.5±16.6b
	Total	26.0±8.1	33.7±9.0	45.3±16.3	56.5±17.1	
PD/richness	Atlantic	0.105±0.013a	0.112±0.012a	0.094±0.009a	0.118±0.012a	0.103±0.014a
	Western Med	0.101±0.013a	0.098±0.009a	0.094±0.006a	0.118±0.015a	0.107±0.019a
	Eastern Med	0.102±0.012a	0.118±0.016a	0.109±0.019b	0.127±0.018b	0.114±0.015b
	Total	0.103±0.012	0.113±0.015	0.100±0.016	0.121±0.017	
Evenness	Atlantic	0.70±0.02a	0.76±0.05a	0.83±0.06ab	0.81±0.04a	0.78±0.06a
	Western Med	0.79±0.04b	0.82±0.02a	0.82±0.02a	0.78±0.03b	0.80±0.04ab
	Eastern Med	0.80±0.03b	0.78±0.06a	0.85±0.02b	0.81±0.04a	0.81±0.04b
	Total	0.78±0.05	0.79±0.05	0.83±0.03	0.80±0.04	
n	Atlantic	8	4	8	13	33
	Western Med	16	9	20	19	64
	Eastern Med	24	12	25	28	89

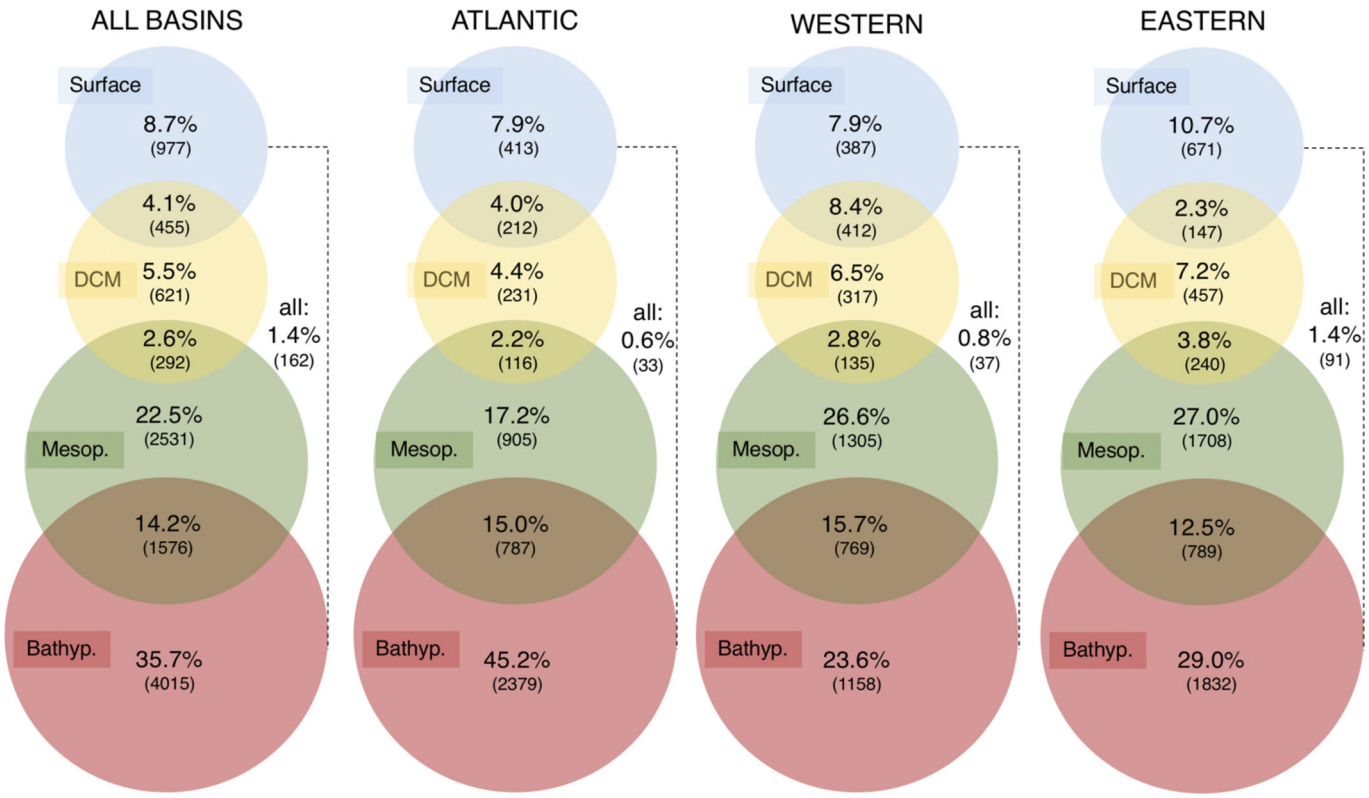

Fig 4. Venn diagram illustrating the % and number (in parenthesis) of ASVs exclusive from each depth layer and those shared between layers. Left: considering all basins. Right: considering each basin separately. ASVs shared by non-consecutive depth layers (e.g., surface and mesopelagic) represented < 6% of all ASVs and are not represented in the diagrams for simplicity.

transect, except for surface Atlantic communities (Fig. 5). However, communities were remarkably heterogeneous among stations at the DCM layer. SAR11 clade bacteria and cyanobacteria dominated both the surface and the DCM communities (Fig. 5), although sharp transitions in the dominance of cyanobacterial genera were observed between the different basins. Whereas *Synechococcus* dominated surface cyanobacterial communities of both Mediterranean basins and the DCM of the Western Mediterranean, *Prochlorococcus* dominated in both surface and DCM in the Atlantic and in the DCM of the Eastern basin (Figs. 5, S4). The mesopelagic and bathypelagic layers were dominated by archaeal ASVs, which comprised roughly half of the 16S sequences (52% and 44% of the communities for the meso- and bathypelagic, respectively; Fig. 5). From these, the majority of sequences corresponded to Thaumarchaeota. The most abundant bacterial groups in the bathypelagic were alpha- and gammaproteobacteria (representing ~ 10% each), followed by members of the phylum Chloroflexi and the SAR406 clade (Marinimicrobia), which represented around 8% of the reads. Specific physical features of the Mediterranean Sea appeared to have a notable impact on the prokaryotic community structure: in Sta. #13–14, located in the Sicily Strait, and #24, at the Eastern side of the Gibraltar Strait, a higher relative abundance of archaea, mostly Thaumarchaeota, could be detected in surface and DCM waters (Fig. 5), reflecting the upward displacement of waters due to the shallow straits.

ANOVA tests using depth layer and basin as factors confirmed the high spatial structuring of many of the taxonomical groups found (Table 2, Table S3). In fact, most of the groups showed significantly different distributions among depth layers (Table 2). For instance, Archaea were predominantly located in the mesopelagic layer, but some archaeal groups were more dominant in the bathypelagic, like the Euryarchaeota Marine Group III or the Woesearchaeota. In contrast, members of the Marine Group I of Thaumarchaeota, like *Candidatus nitrosopumilus*, were enriched at the DCM.

Some bacterial phyla were predominantly found in the euphotic layers (Table 2), like Actinobacteria and Planctomycetes (enriched in DCM waters), Bacteroidetes (both surface and DCM), and Verrucomicrobia, with the exception of the Artic97B-4 marine group. Alphaproteobacteria overall dominated the prokaryotic communities of the surface layer, but there were contrasting patterns within this class. The orders Rhodobacterales, Rickettsiales, and SAR11 bacteria showed a preference for the surface (Table 2), except the deep SAR11 clade that was predominantly found in the mesopelagic, whereas Caulobacterales, Rhodospirillales, and

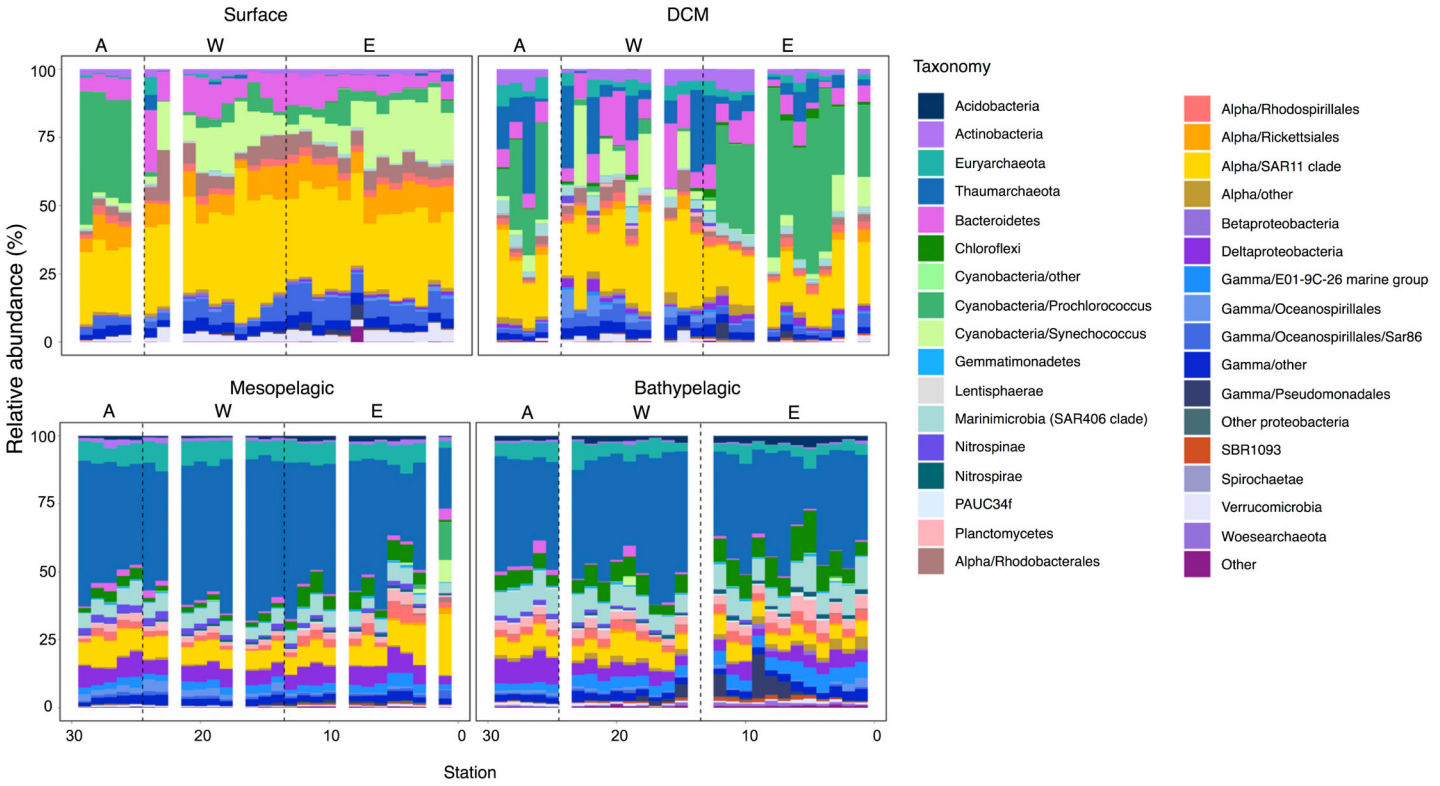

Fig 5. Taxonomic composition of prokaryotic communities across the Mediterranean Sea. Each panel corresponds to one depth layer (S, surface; DCM, deep chlorophyll maxima; M, Mesopelagic; B, Bathypelagic) while stations are organized in columns according to their geographical position (from east to west). Black vertical lines separate ocean basins: North Eastern Atlantic (A), Western Mediterranean (W), Eastern Mediterranean (E).

Sphingomonadales were more frequently found in the bathypelagic. Within the Gammaproteobacteria, the orders Cellvibrionales, the KI89A clade, and the SAR86 were mostly found in surface waters, whereas Alteromonadales, E01-9C-26 marine group, Pseudomonadales, and Xanthomonadales increased their relative abundance in bathypelagic waters. Other phyla were predominantly observed in the deep-water layers, such as Marinimicrobia, Gemmatimonadetes, Lentisphaerae, Nitrospina (higher at the mesopelagic), and Nitrospira (higher at the bathypelagic).

Besides the clear vertical structuring, we also detected horizontal structuring (i.e., differences among basins) for some groups. For instance, SAR324 bacteria and Lentisphaerae displayed higher relative abundances in the Eastern North Atlantic (Tables 2, S3), whereas the relative abundance of Acidobacteria, Chloroflexi, and phylum SBR1093 and the group E01-9c-26 from Gammaproteobacteria increased significantly in the Eastern Mediterranean (Table 2; Fig. S5). Nitrospina showed comparatively higher abundances in the Atlantic and Western Mediterranean basins than in the Eastern Mediterranean basin, while Nitrospira displayed the opposite pattern (Table 2; Fig. S5). Overall, many of the groups that presented changes in abundance among basins were significantly enriched in the dark ocean (Table 2), although there were also some clear segregations in the surface, as for example Surface 2 group of the SAR11 clade, which was overrepresented in the Eastern Mediterranean basin (Table 2; Fig. S6).

Biogeographical barriers in the Mediterranean define different prokaryotic communities in surface and bathypelagic waters

In order to further explore to which extent each basin contained specific prokaryotic taxa, we performed an indicator taxa (at the ASV level) analysis (see the Methods section) for each of the depth layers separately. The number of indicator ASVs and their contribution to the prokaryotic communities was notably higher in the surface and bathypelagic layers than in the DCM or mesopelagic (Fig. 6). Atlantic indicator taxa accounted for $\sim$ 60% and up to 80% of the communities in surface and bathypelagic waters of the Eastern North Atlantic basin, respectively, decreasing sharply at the Mediterranean Sea waters interface. The transition between Mediterranean Sea basins was less abrupt, with Western ASVs gradually being replaced by Eastern Mediterranean ASVs (Fig. 6). Yet, the contribution of Western Mediterranean and Eastern Mediterranean indicator ASVs to surface and bathypelagic communities of the Western and Eastern basins, respectively, was still high, representing up to 50% of the communities. In contrast to surface and bathypelagic layers, there were few indicator ASVs in the

Table 2. Vertical and basin segregation of prokaryotic groups in the Mediterranean Sea. Relative abundance (in %) and results of ANOVA + post hoc Tukey tests looking for significant differences among depth layer or basins. Only those taxa with a different spatial structuring than the group they belong to are listed. Color code denotes the results of the post hoc Tukey tests (see legend below) with darker colors representing significantly higher relative abundances. Light blue shading indicates those groups that displayed abundances higher than 1%.

	Layer effect						Basin effect			
	Average %	ANOVA *P*	S	DCM	M	B	ANOVA *P*	ATL	W	E
Archaea	30.96	<0.0001					ns			
Euryarchaeota	4.21	<0.0001					0.016			
Thermoplasmata	4.19	<0.0001					0.015			
Marine_Group_II	3.16	<0.0001					0.002			
Marine_Group_III	1.03	<0.0001					ns			
Thaumarchaeota	26.45	<0.0001					"			
Marine_Benthic_Group_A	0.47	<0.0001					"			
Marine_Group_I	25.91	<0.0001					"			
Candidatus_Nitrosopelagicus	2.86	<0.0001					"			
Candidatus_Nitrosopumilus	0.76	<0.0001					"			
Woesearchaeota_(DHVEG-6)	0.26	<0.0001					"			
WSA2	0.01	<0.0001					"			
Bacteria	69.04	<0.0001					"			
Acidobacteria	1.10	<0.0001					0.036			
Actinobacteria	1.59	<0.0001					ns			
Bacteroidetes	4.13	<0.0001					"			
Flavobacteriia	3.45	<0.0001					0.037			
Flavobacteriales	3.45	<0.0001					0.037			
Chloroflexi	3.68	<0.0001					0.006			
SAR202_clade	3.49	<0.0001					0.005			
Cyanobacteria	9.68	<0.0001					0.038			
Prochlorococcus	5.64	<0.0001					<0.0001			
Synechococcus	4.00	<0.0001					0.019			
Gemmatimonadetes	0.39	<0.0001					ns			
Lentisphaerae	0.07	<0.0001					0.000			
Marinimicrobia_(SAR406_clade)	4.90	<0.0001					ns			
Nitrospinae	1.27	<0.0001					"			
Nitrospinia	0.76	<0.0001					<0.0001			
Nitrospira	0.45	<0.0001					<0.0001			
PAUC34f	0.27	<0.0001					ns			
Planctomycetes	1.91	<0.0001					"			
Proteobacteria	38.01	<0.0001					"			
AEGEAN-245	0.07	<0.0001					"			
Alphaproteobacteria	24.12	<0.0001					"			
Caulobacterales	0.06	<0.0001					0.015			
Rhizobiales	0.60	<0.0001					ns			
Rhodobacterales	1.90	<0.0001					ns			
Rhodospirillales	1.66	<0.0001					0.005			
Rickettsiales	2.84	<0.0001					"			
SAR116_clade	2.26	<0.0001					"			
SAR11_clade	15.62	<0.0001					"			
Deep_1	2.40	<0.0001					"			
Surface_1	11.20	<0.0001					"			
Surface_2	1.23	<0.0001					0.049			
Surface_4	0.46	<0.0001					ns			
Sphingomonadales	0.43	<0.0001					ns			
Betaproteobacteria	0.27	0.0004					"			
Deltaproteobacteria	3.90	<0.0001					0.071			
SAR324_clade(Marine_group_B)	3.46	<0.0001					0.003			
Gammaproteobacteria	9.55	0.0054					<0.0001			
Alteromonadales	0.29	<0.0001					ns			
Cellvibrionales	0.52	<0.0001					"			
E01-9C-26_marine_group	2.35	<0.0001					0.035			
KI89A_clade	0.31	<0.0001					ns			
Oceanospirillales	3.40	<0.0001					"			
SAR86_clade	2.34	<0.0001					0.037			
Pseudomonadales	0.93	0.017					0.015			
Salinisphaerales	0.87	<0.0001					0.021			
Thiotrichales	0.33	<0.0001					ns			
Vibrionales	0.01	0.0015					0.037			
Xanthomonadales	0.29	<0.0001					ns			
SBR1093	0.36	<0.0001					<0.0001			
Spirochaetae	0.03	<0.0001					ns			
Verrucomicrobia	1.32	<0.0001					ns			
Arctic97B-4_marine_group	0.35	<0.0001					0.040			

A	AB	B	BC	C	CD	D

DCM and mesopelagic layers (Fig. 6) that generally accounted for < 10% of the communities. An exception was the mesopelagic Western Mediterranean indicators, which comprised around 25% of mesopelagic communities in this basin.

sPLS regression analysis unveiled strong associations between abundant (representing 1% of the sequences in at least one sample) surface and bathypelagic basin indicator ASVs and some environmental variables, particularly in the Western and Eastern Mediterranean (Figs. S7, S8). Surface Western Mediterranean indicators were associated with comparatively higher values of photic integrated inorganic nutrients, FDOM (Peaks T and C), the spectral slope of CDOM between 275 and 295 nm (i.e., lower molecular weight of CDOM compounds; Helms et al. 2008), dissolved oxygen, particulate carbon, and PA, and negatively associated to temperature and the proportion of labile to recalcitrant compounds (FDOM peak T to peak C ratio). Conversely, Eastern Mediterranean indicators displayed the opposite associations. Surface Atlantic indicator ASVs were associated with relatively warmer waters. These Atlantic indicator ASVs were mostly represented by *Prochlorococcus*, which decreased sharply in relative abundance in the Western basin (Figs. S7, S9). In contrast, Western indicators included *Synechococcus*, Flavobacteriales and SAR11 surface clade 1 ASVs. Eastern indicators comprised other *Synechococcus* and SAR11 surface clade 1 ASVs, as well as several SAR116 ASVs and members of the SAR86 clade (Figs. S7, S9).

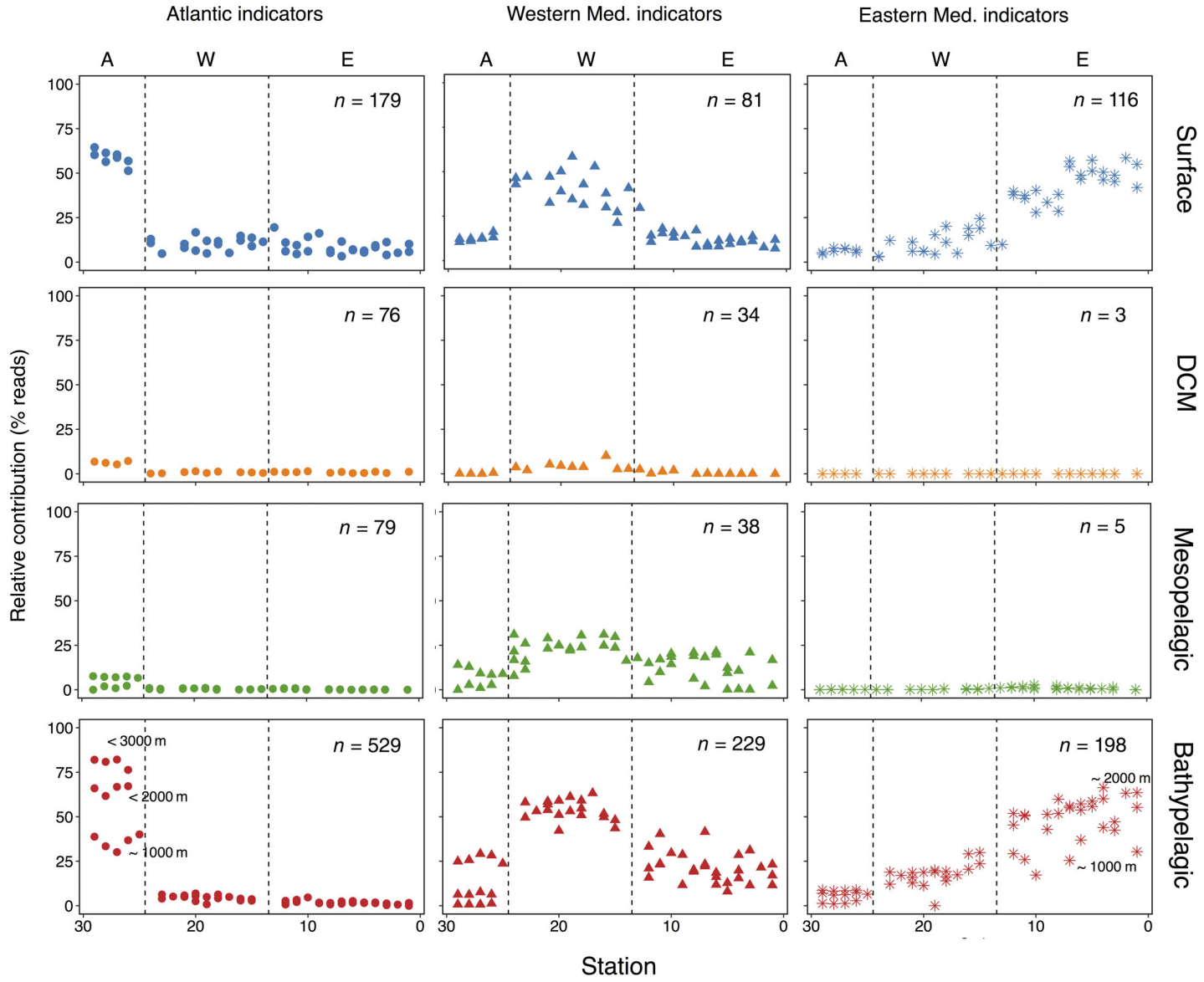

Fig 6. Contribution of basin indicator ASVs to the prokaryotic communities in each of the depth layers. Basins are separated by a vertical dashed line. Left panel: Atlantic indicators. Mid-panel: Western Mediterranean indicators. Right panel: Eastern Mediterranean indicators. The *n* value within each plot represents the number of indicator ASVs per layer and basin.

In the bathypelagic layer, the basin indicators were also associated with different environmental variables (Fig. S8). Bathypelagic Atlantic indicators were linked to cold temperatures, and increasing values of inorganic nutrient concentrations, humic-like FDOM (peak C), the spectral slope of CDOM between 275 and 295 nm, high apparent oxygen utilization, and the proportion of high nucleic acid bacteria, whereas Eastern indicators displayed the opposite trend (Fig. S8). Indicators from the Western basin showed in general weaker associations with environmental variables but were linked to overall comparatively higher PAs. Thaumarchaeota represented a large fraction of bathypelagic indicators in the three basins, but in the Western Mediterranean they accounted for most of the indicator sequences (Fig. S9).

Discussion

Our study represents the first quasi-synoptic overview of prokaryotic diversity and community composition along an east–west transect in the Mediterranean Sea. This miniature ocean is characterized by a marked horizontal gradient in surface nutrient availability, decreasing from west to east (Figs. 1B, S1C). Moreover, the Gibraltar and Sicily straits act as physical obstacles that reduce circulation and water mass mixing across basins in the bathypelagic. Taken together, these characteristics lead to a high spatial structuring of prokaryotic communities. This structuring is reflected by the differences in diversity, community structure, and composition in both the vertical and horizontal dimensions.

Prokaryotic communities are highly structured along the vertical axis

The marked vertical structuring observed agrees with previous local studies in the Mediterranean Sea (Ghiglione et al. 2008; Crespo et al. 2013; Techtmann et al. 2015; Mestre et al. 2017) and elsewhere (Schattenhofer et al. 2009; Sunagawa et al. 2015) showing a dominance of SAR11 and Bacteroidetes in euphotic layers (Ghiglione et al. 2008; Crespo et al. 2013; Techtmann et al. 2015; Mestre et al. 2017) and the presence of Thaumarchaeota, SAR324, and SAR202 among other groups, in deep waters (Karner et al. 2001; Techtmann et al. 2015; Severin et al. 2016). The vertical segregation within the Archaea also agrees with previous findings, showing that the Marine Group I Thaumarchaeota are more prevalent in the mesopelagic layer (Santoro et al. 2019), and Marine Group III in the bathypelagic layer (Martin-Cuadrado et al. 2008; Li et al. 2015). Marine Group II archaea were significantly enriched in the mesopelagic in our study, although they have been reported to be most abundant in sunlit waters in other regions of the ocean, as the North Pacific (Massana et al. 1997; DeLong et al. 2006). Different environmental conditions in the Mediterranean could lead to the presence of different Marine Group II ecotypes (Pereira et al. 2019) with a preference for mesopelagic waters. Woesearchaeota are found in low abundance in a wide variety of environments (Liu et al. 2018) but in our study they were significantly enriched in the bathypelagic. The abundance of WSA2 Archaea, which have been reported to possess energy conservation mechanisms (Nobu et al. 2016), also increased in the bathypelagic. Besides the observed changes in the vertical distribution of prokaryotic groups, our broad-scale spatial resolution allowed us to explore how this vertical structuring changed from east to west and how it compares with the adjacent Atlantic waters, looking for the particularities of each basin.

Prokaryotic richness increased with depth (Fig. 3), in line with previous studies performed in the Atlantic Ocean (Agogué et al. 2011; Frank et al. 2016), the Mediterranean Sea (Pommier et al. 2010; Luna 2014; Techtmann et al. 2015; Severin et al. 2016; Mestre et al. 2017), or in global ocean waters (Sunagawa et al. 2015). This increase in richness was caused by a high number of ASVs exclusively found in deep layers (Fig. 4), and to an increased contribution of rare members in the deep ocean communities (Fig. S10). Conversely, lower diversity and few exclusive ASVs were found in the euphotic layer, which were dominated by several SAR11 and cyanobacterial ASVs and displayed comparatively a reduced rare biosphere in all three basins (Fig. S10). Rare prokaryotes have been shown to guarantee the metabolic potential of deep ocean microbial communities in the absence of fresh carbon inputs (Sebastián et al. 2018), which may explain why deep waters harbor a larger rare biosphere. The existence of a diverse microbial community ensures the potential to quickly exploit sudden increases in substrates associated to active transport by migrating animals (Steinberg et al. 2000; Calleja et al. 2018; Hernández-León et al. 2019), sinking particles arriving to deep waters (Smith et al. 2018), or deep-water formation events (Tamburini et al. 2013; Luna et al. 2016; Severin et al. 2016).

Richness and PD decreased from the Atlantic to the Eastern Mediterranean regardless of the depth layer. However, while in the epipelagic and the mesopelagic, they did not correlate with any of the environmental variables tested (Table S2), in the bathypelagic they were significantly correlated with the concentration of organic carbon, inorganic nutrients, and humic-like FDOM peak C. This suggests that deep waters with increased resource availability (i.e., in the Atlantic) sustain more diverse communities, or alternatively that richer communities might transform the available organic carbon into less available humic by-products, in what is called the microbial carbon pump (Jiao et al. 2010). The reason why we did not observe any correlation between diversity and environmental variables in the mesopelagic may be the fact that this layer spans a transition from epipelagic waters (hence illuminated and influenced by primary production) to deep waters (thus dark, nutrient-enriched, cold, and high-pressure dominated), and therefore, likely comprises a wide variety of habitats. In fact, in the Mediterranean Sea, samples that are globally defined as mesopelagic (from 200 to 1000 m) comprise not only intermediate but also deep-water masses (Catalá et al. 2018). To explore the hypothesis that the mesopelagic layer comprised a wide variety of niches, we calculated the coefficient of variation of several environmental

parameters along the four depth layers (surface, DCM, meso- and bathypelagic; Fig. S11) and observed that mesopelagic waters displayed the highest variability in the variables related to particle organic matter pools (POC, PON, and TEP), suggesting a broad variation range in particle abundance and quality. Despite the lack of correlation with environmental variables, the high richness observed in this layer agrees with previous findings (Sunagawa et al. 2015) and with the idea that the mesopelagic is a hotspot for microbial diversity and activity (Arístegui 2005; Calleja et al. 2018).

The most oligotrophic waters (i.e., the Eastern Mediterranean) displayed communities with higher PD/richness ratios (Fig. S2), which were also negatively correlated with the concentration of organic carbon in deep waters (Table S2). One could hypothesize that oligotrophic waters favor the coexistence of more phylogenetically diverse phylotypes despite harboring globally less diverse communities, implying less microdiversity. Although not many studies have addressed this issue, these findings contrast with previous results obtained in a mesocosm study showing that taxa tended to be more distantly related at higher ecosystem productivities (Horner-Devine and Bohannan 2006). Given that closely related taxa seem to be more functionally similar than distantly related taxa (Bryant et al. 2012), the relative diversification we observed in Eastern waters may be a consequence of competitive exclusion between closely related taxa (Cavender-Bares and Wilczek 2003) facing poor trophic conditions. Nonetheless, further studies looking at the genetic repertoire and functional redundancy of prokaryotic communities could help to gain a clearer insight into how microbial communities structure across distinct trophic gradients.

Prokaryotic communities are horizontally structured across the Mediterranean Sea

Besides the high structuring in the vertical dimension, our analyses revealed also a clear spatial structuring in the horizontal dimension, particularly in the surface and the bathypelagic layers (Table 2; Fig. 6).

In surface waters, Atlantic indicator ASVs were abruptly substituted by Mediterranean ASVs, and we could document a gradual exchange of ASVs across the W–E transect (Fig. 6). The sharp decrease in the contribution of Atlantic indicator taxa at the interface of Mediterranean waters was mostly driven by the disappearance of *Prochlorococcus* in surface waters (Fig. S9). Eastern indicators were associated with lower values of photic-zone integrated nutrients (Fig. S7), which agrees with the known west to east gradient of increasing oligotrophy, and the strong phosphorus limitation in Eastern Mediterranean waters (Thingstad et al. 2005). This gradient was also reflected in the distribution of SAR11 populations: even though SAR11 are the most abundant taxa everywhere in the epipelagic, there was a spatial structuring of different surface clades. For instance, the surface 1 clade of SAR11 was mostly present in the Western Mediterranean while the surface 2 clade was mostly seen in the Eastern Mediterranean (Fig. S6). Even within surface 1 clade, different ASVs appear as indicators of the different basins (Fig. S7). Indeed, previous studies have already pointed out the importance of P limitation as a selective force shaping the biogeography of distinct SAR11 clades (Coleman and Chisolm 2010; Salter et al. 2014). Cyanobacteria also presented a high degree of spatial structuring within the Mediterranean: while *Synechococcus* were mostly present in the surface of the Levantine basin (Eastern Mediterranean), *Prochlorococcus* appeared deeper, at around 100 m deep (Fig. S4). This vertical segregation in the Levantine basin is in line with previous studies (Techtmann et al. 2015), and agrees with the idea that *Synechococcus* grow better at low nutrients and high light levels (Agawin et al. 1998; Nunes et al. 2018), while *Prochlorococcus* dominates at lower light levels. Notably, Cyanobacteria were less abundant overall in the Western Mediterranean, coinciding with those stations with higher Chl *a* concentration (Martínez-Pérez et al. 2017), which may indicate that these waters were dominated by eukaryotic phytoplankton (Arístegui, Gasol et al. unpubl.). However, these groups may display strong seasonality (Malmstrom et al. 2010), so the patterns observed here could be different in other times of the year (Mena et al. 2020).

The practically absence of basin DCM indicators may be due to the fact that this structure is highly heterogeneous at a fine vertical spatial scale (Latasa et al. 2016; Haro-Moreno et al. 2018), as reflected by the variable taxonomic composition observed along the transect (Fig. 5). Nonetheless, despite the lack of horizontal structuring between the different basins, we found some groups to be preferentially enriched in this layer. One clear example is the OM1 clade of Actinobacteria (Table 2). This clade was first described in the Western Mediterranean (*Candidatus* Actinomarina; Ghai et al. 2013), but in our study it also accounted for a large share of microbial community composition in the Eastern basin near the strait of Sicily and in the Atlantic basin (Fig. S12).

Mesopelagic prokaryotic communities were also poorly structured throughout the basins, as indicator ASVs were few and always showed low relative abundances along the transect, except for a slight increase in the Western basin (Fig. 6). Besides the presence of different intermediate and deep-water masses in our mesopelagic samples, the ubiquitous distribution of mesopelagic ASVs may be due to the fact that the Mediterranean mesopelagic is connected through the Levantine Intermediate Water (LIW), a water mass formed in the Eastern basin that reaches 200–500 m depth (Malanotte-Rizzoli and Hecht 1988; Catalá et al. 2018), and travels west, flowing cyclonically in the Western basin while being progressively mixed with surrounding waters until it exits the Mediterranean Sea through the strait of Gibraltar (Emelianov et al. 2006). Hence, the LIW connects all Mediterranean Sea mesopelagic waters, presumably also connecting their prokaryotic communities and thus erasing biogeographical barriers. The LIW also transports DOM that is progressively consumed by prokaryotes (Martínez-Pérez

et al. 2017), thus Western Mediterranean mesopelagic waters hold more refractory low-molecular weight DOM that could select for specific ASVs degrading it. This may be a reason for the increase in the relative abundance of mesopelagic indicators observed in this basin (Fig. 6).

As opposed to DCM and mesopelagic communities, there was a marked horizontal structuring of bathypelagic communities, mostly between the Atlantic and the Mediterranean basins, as indicated by the high percentage of exclusive ASVs in the Atlantic (Fig. 4) and the sharp changes in the contribution of basin indicator ASVs when crossing the strait of Gibraltar (Fig. 6). This shows that the shallow Gibraltar and Sicily straits act as physical barriers that prevent the direct mixing and spreading of the deep-water bodies in the Mediterranean (Astraldi et al. 1999), creating unique environments that lead to the ecological selection of specialized taxa. In fact, closely related phylotypes appeared as indicators of the different basins (Fig. S8), suggesting a fine-tuning of metabolic capacities among closely related microbes facing the different environmental conditions of the isolated water masses within each basin, as has been proposed to explain prokaryote niche partitioning in other systems (Carlson et al. 2008; Hehemann et al. 2016). Temperature has been found to be one of the most determinant factors in the ecological selection of prokaryotes (Sunagawa et al. 2015; Milici et al. 2016), and bathypelagic Atlantic waters are characterized by temperatures $\sim 9^{\circ}$C colder than bathypelagic Mediterranean waters. Thus, it is likely that the segregation of taxa between the Atlantic and the Mediterranean is due to the drastic change in temperature, as hinted by the sPLS analyses (Fig. S8). Between the Mediterranean basins, other environmental factors such as the amount of organic carbon that reaches deep-water layers or the quality of the DOM may play a role, as depicted by the association of Eastern basin bathypelagic indicators with comparatively lower amount of TOC and higher molecular weight of its compounds (lower S275–295 CDOM spectral slope, (Helms et al. 2008; Catalá et al. 2018) (Fig. S8).

Zooming in the meso- and bathypelagic layers, some prokaryotic groups were particularly enriched in the Atlantic Ocean (Table 2), such as Lentisphaerae, or the Arctic 97B-4 marine group of Verrucomicrobia. Lentisphaerae have been described to be exopolymer particle producers (Cho et al. 2004), and higher proportions of exopolymer particles have been reported in the deep Atlantic Ocean compared to the deep Mediterranean Sea (Ortega-Retuerta et al. 2019). SAR324 bacteria were also enriched in the Atlantic meso- and bathypelagic, but were abundant in the mesopelagic layer of the Eastern Mediterranean basin (Fig. S5). The later observation is in line with a previous study that proposed SAR324 as indicative prokaryotes of the LIW in this area (Techtmann et al. 2015). This group is characterized by high metabolic versatility, being able to fix carbon with the energy derived from sulfur oxidation but also being capable of hydrocarbon oxidation (Swan et al. 2011; Sheik et al. 2014). Remarkable trends were observed in the distribution of the nitrite oxidizers across the Mediterranean Sea, with *Nitrospina* showing higher relative abundances throughout the dark waters of the Atlantic and the mesopelagic of the Western Mediterranean, and *Nitrospira* displaying higher relative abundances in the dark waters of the Eastern Mediterranean basin (Fig. S5). Members of these groups play an important role in carbon fixation in the deep ocean (Pachiadaki et al. 2017), but their contrasting biogeography suggests they are governed by different selective forces (Nunoura et al. 2015; Hou et al. 2018).

Among the taxonomic groups that were relatively enriched in the dark waters of the Eastern Mediterranean Sea (Table 2; Fig. S5), we underline the *Gammaproteobacteria* group E01-9C-26, with no cultured representatives but potential versatile methylotrophs and dissimilatory sulfate reducers as hinted by single cell genomics (Landry et al. 2018) and the Chloroflexi-related SAR202 group, frequently observed in deep-water samples (Severin et al. 2016) and in the Eastern Mediterranean Sea (Mehrshad et al. 2018). SAR202 are potential sulfite oxidizers that may use recalcitrant carbon substrates (Landry et al. 2017, 2018; Liu et al. 2020). Given the oligotrophic character of Eastern Mediterranean waters, one could hypothesize that the "hostile" conditions in the carbon-limited bathypelagic would promote a higher diversification of prokaryotic metabolisms, something that will need to be examined in future studies.

Our study presents a quasi-synoptic view of prokaryotic diversity across the Mediterranean Sea and the nearby Atlantic Ocean. It clearly identifies a strong biogeographical spatial structuring, and a large differentiation not only between depth layers but also between basins. This structuring is stronger in the surface and in the bathypelagic layers, pointing to the existence of biogeographic barriers within these layers that are likely caused by the oligotrophic gradient in the surface and the isolation of the bathypelagic water bodies at the Gibraltar and Sicily straits. Our sampling was performed during mid spring (May 2014) when stratification starts to strengthen and the temperature and light increase culminates in the early spring phytoplankton blooms that vary strongly in timing and magnitude in different basins of the Mediterranean Sea (Lazzari et al. 2012). It is thus plausible that the basin and vertical structuring of prokaryotic communities is even stronger in late spring and summer, when oligotrophy becomes more intense and organic matter production feeding the deep-sea microbes is scarcer. Likewise, mixing and deep-water formation events in winter could lead to DOC export to the mesopelagic and sometimes down to the bathypelagic (*see* Santinelli et al. 2015 and references therein). This, together with seasonal changes in the intensity of the inflows of LIW through the Strait of Sicily and Atlantic water through the Strait of Gibraltar (Manzella and La Violette 1990), could also drive changes in the spatial and vertical structuring of prokaryotic communities. Hence, the biogeographic patterns evidenced here should serve as basis for further detailed

studies on prokaryotic community structure in the Mediterranean and other ocean basins, the environmental factors driving this structure, and how it varies over time, as well as on the impact of this regionalization in the function of prokaryotic communities.

References

Agawin, N. S. R., C. M. Duarte, and S. Agustí. 1998. Growth and abundance of *Synechococcus* sp. in a Mediterranean Bay: Seasonality and relationship with temperature. Mar. Ecol. Progr. Ser. **170**: 45–53.

Agogué, H., D. Lamy, P. Neal, M. Sogin, and G. Herndl. 2011. Water mass-specificity of bacterial communities in the North Atlantic revealed by massively parallel sequencing. Mol. Ecol. **20**: 258–274.

Arístegui, J. 2005. Active mesopelagic prokaryotes support high respiration in the subtropical northeast Atlantic Ocean. Geophys. Res. Lett. **32**: 1–4. doi:10.1029/2004gl021863

Arístegui, J., J. M. Gasol, C. M. Duarte, and G. J. Herndl. 2009. Microbial oceanography of the dark ocean's pelagic realm. Limnol. Oceanogr. **54**: 1501–1529.

Astraldi, M., and others. 1999. The role of straits and channels in understanding the characteristics of Mediterranean circulation. Prog. Oceanogr. Ser. **44**: 65–108.

Baltar, F., and J. Arístegui. 2017. Fronts at the surface ocean can shape distinct regions of microbial activity and community assemblages down to the bathypelagic zone: The Azores front as a case study. Front. Mar. Sci. **4**. doi:10.3389/fmars.2017.00252

Benjamini, Y., and Y. Hochberg. 1995. Controlling the false discovery rate: A practical and powerful approach to multiple testing. J. R. Stat. Soc. Ser. B **57**: 289–300. doi:10.1111/j.2517-6161.1995.tb02031.x

Bethoux, J. P., B. Gentili, P. Morin, E. Nicolas, C. Pierre, and D. Ruiz-Pino. 1999. The Mediterranean Sea: A miniature ocean for climatic and environmental studies and a key for the climatic functioning of the North Atlantic. Prog. Oceanogr. **44**: 131–146.

Bryant, J. A., F. J. Stewart, J. M. Eppley, and E. F. DeLong. 2012. Microbial community phylogenetic and trait diversity declines with depth in a marine oxygen minimum zone. Ecology **93**: 1659–1673. doi:10.1890/11-1204.1

Calleja, M. L., M. I. Ansari, A. Røstad, L. Silva, S. Kaartvedt, X. Irigoien, and X. A. G. Morán. 2018. The mesopelagic scattering layer: A hotspot for heterotrophic prokaryotes in the Red Sea twilight zone. Front. Mar. Sci. **5**: 259. doi:10.3389/fmars.2018.00259

Callahan, B. J., P. J. McMurdie, M. J. Rosen, A. W. Han, A. J. A. Johnson, and S. P. Holmes. 2016. DADA2: High-resolution sample inference from Illumina amplicon data. Nat. Methods **13**: 581–583. doi:10.1038/nmeth.3869

Carlson, C. A., R. Morris, R. Parsons, A. H. Treusch, S. J. Giovannoni, and K. Vergin. 2008. Seasonal dynamics of SAR11 populations in the euphotic and mesopelagic zones of the northwestern Sargasso Sea. ISME J. **3**: 283–295. doi:10.1038/ismej.2008.117

Catalá, T. S., and others. 2018. Dissolved organic matter (DOM) in the open Mediterranean Sea. I. Basin–wide distribution and drivers of chromophoric DOM. Prog. Oceanogr. **165**: 35–51. doi:10.1016/j.pocean.2018.05.002

Cavender-Bares, J., and A. Wilczek. 2003. Integrating micro- and macroevolutionary processes in community ecology. Ecology **84**: 592–597.

Celussi, M., and others. 2018. Planktonic prokaryote and protist communities in a submarine canyon system in the Ligurian Sea (NW Mediterranean). Prog. Oceanogr. **168**: 210–221. doi:10.1016/j.pocean.2018.10.002

Cho, J.-C., K. L. Vergin, R. M. Morris, and S. J. Giovannoni. 2004. *Lentisphaera araneosa* gen. nov., sp. nov, a transparent exopolymer producing marine bacterium, and the description of a novel bacterial phylum, Lentisphaerae. Environ. Microbiol. **6**: 611–621. doi:10.1111/j.1462-2920.2004.00614.x

Christensen, J. P., T. T. Packard, F. Q. Dortch, H. J. Minas, J. C. Gascard, C. Richez, and P. C. Garfield. 1989. Carbon oxidation in the deep Mediterranean Sea: Evidence for dissolved organic carbon source. Global Biogeochem. Cycles **3**: 315–335.

Coleman, M. L., and S. W. Chisolm. 2010. Ecosystem-specific selection pressures revealed through comparative population genomics. Proc. Natl. Acad. Sci. USA **107**: 18634–18639.

Crespo, B. G., T. Pommier, B. Fernandez-Gomez, and C. Pedros-Alio. 2013. Taxonomic composition of the particle-attached and free-living bacterial assemblages in the Northwest Mediterranean Sea analyzed by pyrosequencing of the 16S rRNA. Microbiologyopen **2**: 541–552. doi:10.1002/mbo3.92

De Corte, D., T. Yokokawa, M. M. Varela, H. Agogue, and G. J. Herndl. 2009. Spatial distribution of bacteria and archaea and amoA gene copy numbers throughout the water column of the eastern Mediterranean Sea. ISME J. **3**: 147–158. doi:10.1038/ismej.2008.94

DeLong, E. F., and others. 2006. Community genomics among stratified microbial assemblages in the ocean's interior. Science **311**: 496–503. doi:10.1126/science.1120250

Emelianov, M., J. Font, A. Turiel, C. Millot, J. Solé, P. M. Poulain, A. Julià, and M. R. Vitrià. 2006. Transformation of levantine intermediate water tracked by MEDARGO floats in the western Mediterranean. Ocean Sci. **2**: 281–290. doi:10.5194/os-2-281-2006

Falkowski, P. G., T. Fenchel, and E. F. Delong. 2008. The microbial engines that drive Earth's biogeochemical cycles. Science **320**: 1034–1039. doi:10.1126/science.1153213

Frank, A. H., J. A. Garcia, G. J. Herndl, and T. Reinthaler. 2016. Connectivity between surface and deep waters determines prokaryotic diversity in the North Atlantic deep water. Environ. Microbiol. **18**: 2052–2063. doi:10.1111/1462-2920.13237

Ghai, R., C. M. Mizuno, A. Picazo, A. Camacho, and F. Rodriguez-Valera. 2013. Metagenomics uncovers a new

group of low GC and ultra-small marine Actinobacteria. Sci. Rep. **3**. doi:10.1038/srep02471

Ghiglione, J. F., and others. 2008. Role of environmental factors for the vertical distribution (0-1000 m) of marine bacterial communities in the NW Mediterranean Sea. Biogeosciences **5**: 1751–1764.

Gilbert, J. A., and others. 2011. Defining seasonal marine microbial community dynamics. ISME J. **6**: 298–308. doi:10.1038/ismej.2011.107

González, I., K.-A. L. Cao, M. J. Davis, and S. Déjean. 2012. Visualising associations between paired 'omics' data sets. BioData Min. **5**: 19. doi:10.1186/1756-0381-5-19

Hanson, C. A., J. A. Fuhrman, M. C. Horner-Devine, and J. B. Martiny. 2012. Beyond biogeographic patterns: Processes shaping the microbial landscape. Nat. Rev. Microbiol. **10**: 497–506. doi:10.1038/nrmicro2795

Haro-Moreno, J. M., M. López-Pérez, J. R. de la Torre, A. Picazo, A. Camacho, and F. Rodriguez-Valera. 2018. Fine metagenomic profile of the Mediterranean stratified and mixed water columns revealed by assembly and recruitment. Microbiome **6**: 128. doi:10.1186/s40168-018-0513-5

Hehemann, J.-H., and others. 2016. Adaptive radiation by waves of gene transfer leads to fine-scale resource partitioning in marine microbes. Nat. Commun. **7**. doi:10.1038/ncomms12860

Helms, J. R., A. Stubbins, J. D. Ritchie, E. Minor, D. J. Kieber, and K. Mopper. 2008. Absorption spectral slopes and slope ratios as indicators of molecular weight, source, and photobleaching of chromophoric dissolved organic matter. Limnol. Oceanogr. **53**: 955–969.

Herlemann, D. P., M. Labrenz, K. Jurgens, S. Bertilsson, J. J. Waniek, and A. F. Andersson. 2011. Transitions in bacterial communities along the 2000 km salinity gradient of the Baltic Sea. ISME J. **5**: 1571–1579. doi:10.1038/ismej.2011.41

Hernández-León, S., M. P. Olivar, M. L. Fernández de Puelles, A. Bode, A. Castellón, C. López-Pérez, V. M. Tuset, and J. I. González-Gordillo. 2019. Zooplankton and micronekton active flux across the tropical and subtropical Atlantic Ocean. Front. Mar. Sci. **6**. doi:10.3389/fmars.2019.00535

Horner-Devine, M. C., and B. J. M. Bohannan. 2006. Phylogenetic clustering and overdispersion in bacterial communities. Ecology **87**: S100–S108 doi:10.1890/0012-9658(2006)87[100:PCAOIB]2.0.CO;2.

Hou, L., X. Xie, X. Wan, S.-J. Kao, N. Jiao, and Y. Zhang. 2018. Niche differentiation of ammonia and nitrite oxidizers along a salinity gradient from the Pearl River estuary to the South China Sea. Biogeosciences **15**: 5169–5187. doi:10.5194/bg-15-5169-2018

Jiao, N., and others. 2010. Microbial production of recalcitrant dissolved organic matter: Long-term carbon storage in the global ocean. Nat. Rev. Microbiol. **8**: 593–599. doi:10.1038/nrmicro2386

Karner, M. B., E. F. DeLong, and D. M. Karl. 2001. Archaeal dominance in the mesopelagic zone of the Pacific Ocean. Nature **409**: 507–509.

Korlević, M., P. Pop Ristova, R. Garić, R. Amann, S. Orlić, and J. E. Kostka. 2015. Bacterial diversity in the south Adriatic Sea during a strong, deep winter convection year. Appl. Environ. Microbiol. **81**: 1715–1726. doi:10.1128/aem.03410-14

Krom, M. D., N. Kress, and S. Brenner. 1991. Phosphorus limitation of primary productivity in the eastern Mediterranean Sea. Limnol. Oceanogr. **36**: 424–432. doi:10.1002/lno.v36.3

Laghdass, M., and others. 2010. Impact of lower salinity waters on bacterial heterotrophic production and community structure in the offshore NW Mediterranean Sea. Environ. Microbiol. Rep. **2**: 761–769. doi:10.1111/j.1758-2229.2010.00181.x

Landry, Z., B. K. Swan, G. J. Herndl, R. Stepanauskas, S. J. Giovannoni, and J. Zhou. 2017. SAR202 genomes from the dark ocean predict pathways for the oxidation of recalcitrant dissolved organic matter. mBio **8**: e00413–17. doi:10.1128/mBio.00413-17

Landry, Z. C., K. Vergin, C. Mannenbach, S. Block, Q. Yang, P. Blainey, C. Carlson, and S. Giovannoni. 2018. Optofluidic single-cell genome amplification of sub-micron bacteria in the ocean subsurface. Front. Microbiol. **9**: 1152. doi:10.3389/fmicb.2018.01152

Latasa, M., A. Gutiérrez-Rodríguez, A. M. M. Cabello, and R. Scharek. 2016. Influence of light and nutrients on the vertical distribution of marine phytoplankton groups in the deep chlorophyll maximum. Sci. Mar. **80**: 57–62. doi:10.3989/scimar.04316.01A

Lazzari, P., C. Solidoro, V. Ibello, S. Salon, A. Teruzzi, K. Béranger, S. Colella, and A. Crise. 2012. Seasonal and interannual variability of plankton chlorophyll and primary production in the Mediterranean Sea: A modelling approach. Biogeosciences **9**: 217–233. doi:10.5194/bg-9-217-2012

Lê Cao, K.-A., D. Rossouw, C. Robert-Granié, and P. Besse. 2008. A Sparse PLS for Variable Selection when Integrating Omics Data. Stat. Appl. Genet. Mol. Biol. **7**. doi:10.2202/1544-6115.1390

Li, M., B. J. Baker, K. Anantharaman, S. Jain, J. A. Breier, and G. J. Dick. 2015. Genomic and transcriptomic evidence for scavenging of diverse organic compounds by widespread deep-sea archaea. Nat. Commun. **6**: 8933. doi:10.1038/ncomms9933

Liu, S., and others. 2020. Different carboxyl-rich alicyclic molecules proxy compounds select distinct bacterioplankton for oxidation of dissolved organic matter in the mesopelagic Sargasso Sea. Limnol. Oceanogr. **65**: 1532–1553. doi:10.1002/lno.11405

Liu, X., and others. 2018. Insights into the ecology, evolution, and metabolism of the widespread Woesearchaeotal lineages. Microbiome **6**: 102. doi:10.1186/s40168-018-0488-2

Luna, G. M. 2014. Diversity of marine microbes in a changing Mediterranean Sea. Rend. Lincei **26**: 49–58. doi:10.1007/s12210-014-0333-x

Luna, G. M., J. Chiggiato, G. M. Quero, K. Schroeder, L. Bongiorni, D. Kalenitchenko, and P. E. Galand. 2016. Dense water plumes modulate richness and productivity of deep sea microbes. Environ. Microbiol. **18**: 4537–4548. doi:10.1111/1462-2920.13510

Malanotte-Rizzoli, P., and A. Hecht. 1988. Large-scale properties of the eastern Mediterranean: A review. Oceanol. Acta **11**: 323–335.

Malmstrom, R. R., A. Coe, G. C. Kettler, A. C. Martiny, J. Frias-Lopez, E. R. Zinser, and S. W. Chisholm. 2010. Temporal dynamics of Prochlorococcus ecotypes in the Atlantic and Pacific oceans. ISME J. **4**: 1252–1264.

Manzella, G. M. R., and P. E. La Violette. 1990. The seasonal variation of water mass content in the western Mediterranean and its relationship with the inflows through the straits of Gibraltar and Sicily. J. Geophys. Res. Oceans **95**: 1623–1626. doi:10.1029/JC095iC02p01623

Mapelli, F., and others. 2013. Biogeography of planktonic bacterial communities across the whole Mediterranean Sea. Ocean Sci. **9**: 585–595. doi:10.5194/os-9-585-2013

Martin-Cuadrado, A.-B., F. Rodriguez-Valera, D. Moreira, J. C. Alba, E. Ivars-Martínez, M. R. Henn, E. Talla, and P. López-García. 2008. Hindsight in the relative abundance, metabolic potential and genome dynamics of uncultivated marine archaea from comparative metagenomic analyses of bathypelagic plankton of different oceanic regions. ISME J. **2**: 865–886. doi:10.1038/ismej.2008.40

Martínez-Pérez, A. M., H. Osterholz, M. Nieto-Cid, M. Álvarez, T. Dittmar, and X. A. Álvarez-Salgado. 2017. Molecular composition of dissolved organic matter in the Mediterranean Sea. Limnol. Oceanogr. **62**: 2699–2712. doi:10.1002/lno.10600

Martínez-Pérez, A. M., and others. 2019. Dissolved organic matter (DOM) in the open Mediterranean Sea. II: Basin–wide distribution and drivers of fluorescent DOM. Prog. Oceanogr. **170**: 93–106. doi:10.1016/j.pocean.2018.10.019

Martin, M. 2011. Cutadapt removes adapter sequences from high-throughput sequencing reads. EMBnet.journal **17**: 10. doi:10.14806/ej.17.1.200

Massana, R., A. E. Murray, C. M. Preston, and E. F. DeLong. 1997. Vertical distribution and phylogenetic characterization of marine planktonic Archaea in the Santa Barbara Channel. Appl. Environ. Microbiol. **63**: 50–56.

Mehrshad, M., F. Rodriguez-Valera, M. A. Amoozegar, P. Lopez-Garcia, and R. Ghai. 2018. The enigmatic SAR202 cluster up close: Shedding light on a globally distributed dark ocean lineage involved in sulfur cycling. ISME J. **12**: 655–668. doi:10.1038/s41396-017-0009-5

Mena, C., P. Reglero, R. Balbín, M. Martín, R. Santiago, and E. Sintes. 2020. Seasonal niche partitioning of surface temperate open ocean prokaryotic communities. Front. Microbiol. **11**. doi:10.3389/fmicb.2020.01749

Mestre, M., I. Ferrera, E. Borrull, E. Ortega-Retuerta, S. Mbedi, H. P. Grossart, J. M. Gasol, and M. M. Sala. 2017. Spatial variability of marine bacterial and archaeal communities along the particulate matter continuum. Mol. Ecol. **26**: 6827–6840. doi:10.1111/mec.14421

Milici, M., and others. 2016. Bacterioplankton biogeography of the Atlantic Ocean: A case study of the distance-decay relationship. Front. Microbiol. **7**. doi:10.3389/fmicb.2016.00590

Morales, S. E., M. Meyer, K. Currie, and F. Baltar. 2018. Are oceanic fronts ecotones? Seasonal changes along the subtropical front show fronts as bacterioplankton transition zones but not diversity hotspots. Environ. Microbiol. Rep. **10**: 184–189. doi:10.1111/1758-2229.12618

Nobu, M. K., T. Narihiro, K. Kuroda, R. Mei, and W.-T. Liu. 2016. Chasing the elusive Euryarchaeota class WSA2: Genomes reveal a uniquely fastidious methyl-reducing methanogen. ISME J. **10**: 2478–2487. doi:10.1038/ismej.2016.33

Nunes, S., M. Latasa, J. M. Gasol, and M. Estrada. 2018. Seasonal and interannual variability of phytoplankton community structure in a Mediterranean coastal site. Mar. Ecol. Prog. Ser. **592**: 57–75. doi:10.3354/meps12493

Nunoura, T., and others. 2015. Hadal biosphere: Insight into the microbial ecosystem in the deepest ocean on Earth. Proc. Natl. Acad. Sci. USA **112**: E1230–E1236. doi:10.1073/pnas.1421816112

Oksanen, J., F. G. Blanchet, R. Kindt, and others. 2015. Vegan: Community Ecology Package. R package version 2.5-5. https://CRAN.R-project.org/package=vegan.

Ortega-Retuerta, E., I. P. Mazuecos, I. Reche, J. M. Gasol, X. A. Álvarez-Salgado, M. Álvarez, M. F. Montero, and J. Arístegui. 2019. Transparent exopolymer particle (TEP) distribution and in situ prokaryotic generation across the deep Mediterranean Sea and nearby north east Atlantic Ocean. Prog. Oceanogr. **173**: 180–191. doi:10.1016/j.pocean.2019.03.002

Pachiadaki, M. G., and others. 2017. Major role of nitrite-oxidizing bacteria in dark ocean carbon fixation. Science **358**: 1046–1051. doi:10.1126/science.aan8260

Parada, A. E., D. M. Needham, and J. A. Fuhrman. 2016. Every base matters: Assessing small subunit rRNA primers for marine microbiomes with mock communities, time series and global field samples. Environ. Microbiol. **18**: 1403–1414. doi:10.1111/1462-2920.13023

Pereira, O., C. Hochart, J. C. Auguet, D. Debroas, and P. E. Galand. 2019. Genomic ecology of marine group II, the most common marine planktonic Archaea across the surface ocean. Microbiologyopen **8**: e00852. doi:10.1002/mbo3.852

Pinhassi, J., and others. 2006. Seasonal changes in bacterioplankton nutrient limitation and their effects on bacterial community composition in the NW Mediterranean Sea. Aquat. Microb. Ecol. **44**: 241–252.

Pommier, T., P. R. Neal, J. M. Gasol, M. Coll, S. G. Acinas, and C. Pedrós-Alió. 2010. Spatial patterns of bacterial richness

and evenness in the NW Mediterranean Sea explored by pyrosequencing of the 16S rRNA. Aquat. Microb. Ecol. **61**: 221–233. doi:10.3354/ame01484

Pulido-Villena, E., J.-F. Ghiglione, E. Ortega-Retuerta, F. V. Wambeke, and T. Zohary. 2012. Heterotrophic bacteria in the pelagic realm of the Mediterranean Sea. *In* N. Stambler [ed.], Life in the Mediterranean Sea: A look into habitat changes. Nova Sciences Publisher.

Roberts, D. W. 2019. labdsv: Ordination and multivariate analysis for ecology.

Rohart, F., B. Gautier, A. Singh, and K.-A. Lê Cao. 2017. mixOmics: An R package for 'omics feature selection and multiple data integration D. Schneidman [ed.]. PLOS Comput. Biol **13**: e1005752. doi:10.1371/journal.pcbi.1005752

Salazar, G., F. M. Cornejo-Castillo, V. Benítez-Barrios, E. Fraile-Nuez, X. A. Álvarez-Salgado, C. M. Duarte, J. M. Gasol, and S. G. Acinas. 2015. Global diversity and biogeography of deep-sea pelagic prokaryotes. ISME J. **10**: 596–608. doi:10.1038/ismej.2015.137

Salter, I., P. E. Galand, S. K. Fagervold, P. Lebaron, I. Obernosterer, M. J. Oliver, M. T. Suzuki, and C. Tricoire. 2014. Seasonal dynamics of active SAR11 ecotypes in the oligotrophic Northwest Mediterranean Sea. ISME J. **9**: 347–360. doi:10.1038/ismej.2014.129

Sammartino, S., J. García-Lafuente, C. Naranjo, J. C. Sánchez-Garrido, R. Sánchez-Leal, and A. Sánchez-Román. 2015. Ten years of marine current measurements in Espartel Sill, Strait of Gibraltar. J. Geophys. Res. Oceans **120**: 6309–6328. doi:10.1002/2014JC010674

Santinelli, C., L. Nannicini, and A. Seritti. 2010. DOC dynamics in the meso and bathypelagic layers of the Mediterranean Sea. Deep-Sea Res. II Top. Stud. Oceanogr. **57**: 1446–1459. doi:10.1016/j.dsr2.2010.02.014

Santinelli, C., C. Follett, S. Retelletti Brogi, L. Xu, and D. Repeta. 2015. Carbon isotope measurements reveal unexpected cycling of dissolved organic matter in the deep Mediterranean Sea. Mar. Chem. **177**: 267–277. doi:10.1016/j.marchem.2015.06.018

Santoro, A. E., R. A. Richter, and C. L. Dupont. 2019. Planktonic marine Archaea. Ann. Rev. Mar. Sci. **11**: 131–158. doi:10.1146/annurev-marine-121916-063141

Schattenhofer, M., B. M. Fuchs, R. Amann, M. V. Zubkov, G. A. Tarran, and J. Pernthaler. 2009. Latitudinal distribution of prokaryotic picoplankton populations in the Atlantic Ocean. Environ. Microbiol. **11**: 2078–2093. doi:10.1111/j.1462-2920.2009.01929.x

Schliep, K. P. 2011. phangorn: Phylogenetic analysis in R. Bioinformatics **27**: 592–593. doi:10.1093/bioinformatics/btq706

Sebastián, M., J.-C. Auguet, C. X. Restrepo-Ortiz, M. M. Sala, C. Marrasé, and J. M. Gasol. 2018. Deep ocean prokaryotic communities are remarkably malleable when facing long-term starvation. Environ. Microbiol. **20**: 713–723. doi:10.1111/1462-2920.14002

Severin, T., and others. 2016. Impact of an intense water column mixing (0-1500 m) on prokaryotic diversity and activities during an open-ocean convection event in the NW Mediterranean Sea. Environ. Microbiol. **18**: 4378–4390. doi:10.1111/1462-2920.13324

Sheik, C. S., S. Jain, and G. J. Dick. 2014. Metabolic flexibility of enigmatic SAR324 revealed through metagenomics and metatranscriptomics. Environ. Microbiol. **16**: 304–317. doi:10.1111/1462-2920.12165

Smith, K. L., H. A. Ruhl, C. L. Huffard, M. Messié, and M. Kahru. 2018. Episodic organic carbon fluxes from surface ocean to abyssal depths during long-term monitoring in NE Pacific. Proc. Natl. Acad. Sci. USA **115**: 12235–12240. doi:10.1073/pnas.1814559115

Steinberg, D. K., C. A. Carlson, N. R. Bates, S. A. Goldthwait, L. P. Madin, and A. F. Michaels. 2000. Zooplankton vertical migration and the active transport of dissolved organic and inorganic carbon in the Sargasso Sea. Deep-Sea Res. I **47**: 137–158.

Sunagawa, S., and others. 2015. Structure and function of the global ocean microbiome. Science **348**: 1261359. doi:10.1126/science.1261359

Swan, B. K., and others. 2011. Potential for chemolithoautotrophy among ubiquitous bacteria lineages in the dark ocean. Science **333**: 1296–1300. doi:10.1126/science.1203690

Tamburini, C., and others. 2013. Deep-Sea bioluminescence blooms after dense water formation at the ocean surface. PLoS One **8**: e67523. doi:10.1371/journal.pone.0067523

Techtmann, S. M., J. L. Fortney, K. A. Ayers, D. C. Joyner, T. D. Linley, S. M. Pfiffner, and T. C. Hazen. 2015. The unique chemistry of eastern Mediterranean water masses selects for distinct microbial communities by depth. PLoS One **10**: e0120605. doi:10.1371/journal.pone.0120605

Thiele, S., M. Richter, C. Balestra, F. O. Glockner, and R. Casotti. 2017. Taxonomic and functional diversity of a coastal planktonic bacterial community in a river-influenced marine area. Mar. Genomics **32**: 61–69. doi:10.1016/j.margen.2016.12.003

Thingstad, T., and others. 2005. Nature of phosphorus limitation in the ultraoligotrophic eastern Mediterranean. Science **309**: 1068–1071.

Thingstad, T. F., U. L. Zweifel, and F. Rassoulzadegan. 1998. P limitation of heterotrophic bacteria and phytoplankton in the northwest Mediterranean. Limnol. Oceanogr. **43**: 88–94.

Wang, Q., G. M. Garrity, J. M. Tiedje, and J. R. Cole. 2007. Naïve Bayesian Classifier for Rapid Assignment of rRNA Sequences into the New Bacterial Taxonomy. Appl. Environ. Microbiol. **73**: 5261–5267. doi:10.1128/AEM.00062-07

Whitman, W. B., D. C. Coleman, and W. J. Wiebe. 1998. Prokaryotes: The unseen majority. Proc. Natl. Acad. Sci. USA **95**: 6578–6583.

Wright, E. 2016. Using DECIPHER v2.0 to analyze big biological sequence data in R. R J. **8**: 352–359.

Yokokawa, T., D. De Corte, E. Sintes, and G. J. Herndl. 2010. Spatial patterns of bacterial abundance, activity and community composition in relation to water masses in the eastern Mediterranean Sea. Aquat. Microb. Ecol. **59**: 185–195. doi:10.3354/ame01393

Acknowledgments

We thank the crew of the R/V "Sarmiento de Gamboa" and the technicians of the Marine Technology Unit for their assistance in the field as well as the MarBits Bioinformatics Platform of the ICM. We also thank V. Vieitez, M.J. Pazó, T.S. Catalá, and X.A. Álvarez-Salgado for providing the data of TOC, FDOM, and CDOM. Sampling was funded by grant HOTMIX (CTM2011-30010/MAR), and processing also by grants REMEI (CTM2015-70340-R) and MIAU (RTI2018-101025-B-I00) from the Spanish Ministry of Science and Innovation, cofunded with FEDER funds. It has also received support from the Spanish government through the "Severo Ochoa Centre of Excellence" accreditation (CEX2019-000928-S) and the Catalan government through excellence group grant 2017SGR/1568. Laura Gómez-Consarnau was funded by grant OCE1924464 from the United States National Science Foundation (NSF).

Conflict of Interest

None declared.

Submitted 07 May 2021
Revised 30 July 2021
Accepted 15 September 2021

Associate editor: Phyllis Lam